ORIGINAL ARTICLE

Bone Augmentation in Rat by Highly Porous β-TCP Scaffolds with Different Open-cell Sizes in Combination with Fibroblast Growth Factor-2

Hirofumi MIYAJI[1], Hiroyuki YOKOYAMA[1], Yuta KOSEN[1], Hiroyuki NISHIMURA[2], Kazuyasu NAKANE[2], Saori TANAKA[1], Kaori OTANI[1], Kana INOUE[1], Asako IBARA[1], Izumi KANAYAMA[1], Takashi YOSHIDA[1], Kosuke OGAWA[1], Erika NISHIDA[1] and Masamitsu KAWANAMI[1]

[1] Department of Periodontology and Endodontology, Hokkaido University Graduate school of dental medicine, Sapporo, Japan
[2] Inoac Corporation, Nagoya, Japan

SYNOPSIS

We prepared highly porous beta-tricalcium phosphate (β-TCP) scaffolds with different open-cell structure sizes. The aim of this study was to examine whether the open-cell size of the scaffold affected osteoinduction in combination with fibroblast growth factor-2 (FGF2) in rats. Polyurethane foam was immersed in β-TCP slurry and sintered in a furnace. Porous β-TCP scaffolds were prepared in three cell sizes (0.6, 0.4 and 0.3 mm) and characterized. Subsequently, each scaffold with FGF2 was implanted to rat cranial bone. Histomorphometric analyses were taken at 35 days post-surgery. The results showed that each β-TCP scaffold exhibited fully interconnected porosity, and frequently allowed bone tissue ingrowth. The 0.4-mm cell sized scaffold significantly promoted bone augmentation compared to the 0.3-mm type. Resorption of the β-TCP scaffold of 0.4-mm cell size was frequently accelerated. In conclusion, FGF2-loaded β-TCP scaffolds with 0.4-mm cell size would be effective for bone tissue engineering.

***Key words**: bone tissue engineering, beta-tricalcium phosphate (β-TCP), regenerative scaffold, fibroblast growth factor-2 (FGF2), open-cell structure*

INTRODUCTION

In tissue engineering therapy, proliferation and migration of regenerated cells should be facilitated to reform functional tissue following surgical treatment. For this objective, three-dimensional scaffolds, an important element of tissue engineering, are being extensively studied for application in regenerative procedures. Bioceramic materials have mechanical, biocompatible and osteoconductive properties for use as scaffolds in various artificially synthesized types and forms, e.g., bioactive glass[1], hydroxyapatite (HA) [2, 3], tricalcium phosphate (TCP) [3, 4] and composites [5, 6]. β-TCP presents a greater biodegradable effect in comparison with HA [7]. The β-TCP scaffold in combination with growth factors has been shown to

stimulate bone augmentation [4, 8, 9]. For clinical trials, bone graft substitutes using β-TCP have been widely used in the orthopedic and dental fields [10,11].

Regenerative scaffolds should induce rapid replacement by reconstructed tissue following implantation to the healing site. Degradation of β-TCP has revealed, however, that resorption of β-TCP is relatively slow compared to bone re-growth [3]. Frequently, a large amount of residual β-TCP is evident in the regenerated tissue [10, 11]. The long-term residue of bioceramics prevents active tissue remodeling, resulting in immature tissue formation [8]. Furthermore, infection risk is increased by residual material exposure. In the current study, we prepared three-dimensional scaffolds with high porosity (>90%) using polyurethane foam with several open-cell structure sizes. Foam-type materials have large inner-spaces and may allow tissue ingrowth and rapid biodegradability.

Growth factors are important elements for promoting proliferation and differentiation of cells in tissue engineering. Fibroblast growth factor-2 (FGF2) enhances cell activities associated with wound healing [12]. FGF2 application to scaffolds could stimulate rapid tissue recreation in the inner space of the scaffold [13]. FGF2 also modulates proliferation and differentiation of osteogenic cells [13-15]. Highly porous β-TCP scaffolds in combination with FGF2 could be a future component of bone tissue engineering.

In general, the morphology of the scaffold plays a key role in bone tissue engineering. Many investigators have reported that adequate porosity and pore size of scaffold promotes osteoconductivity [16, 17]. The interconnected structure of the bioceramic scaffold was associated with cell growth and differentiation [18]. We hypothesized that FGF2-loaded β-TCP scaffolds could stimulate bone augmentation. However, the relationship between FGF2 use and the open-cell structure of highly porous β-TCP scaffolds has not been investigated to date. Accordingly, the aim of the present study was to examine whether the open-cell size of the β-TCP scaffold could affect bone augmentation in rats using FGF2.

MATERIALS AND METHODS

Preparation of β-TCP scaffold

β-TCP slurry was prepared from β-TCP powder (average particle size: 2.3 μm) provided by Tomita Pharmaceuticals (Naruto, Japan). Three open-cell types of polyurethane foam (MF-13, -20 and -30, Inoac Corporation, Nagoya, Japan) were cut and immersed in homogeneous β-TCP slurry. After drying, the foam was sintered in a furnace (1,150 °C).

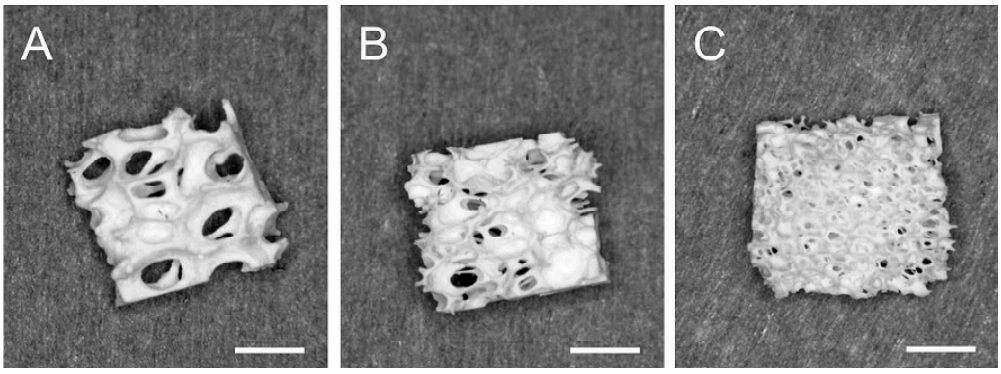

Figure 1
Photographs of highly porous β-TCP scaffolds. A: 0.6-, B: 0.4-, C: 0.3-mm cell type. Different open-cell structures were exhibited. Scale bars represent 1 mm.

Porous β-TCP scaffolds were prepared in three cell sizes (0.6, 0.4 and 0.3 mm) and had a highly interconnected structure with open-cells (Fig.1).

Evaluation of scaffold characteristics

The structures of the β-TCP scaffolds were examined using a scanning electron microscope (SEM, JSM-7600F, JEOL, Tokyo, Japan) at an accelerating voltage of 1 kV after carbon coating. After embedding the β-TCP scaffold in epoxy resin, the cut surface was also scanned. The porosity of the β-TCP scaffold was calculated according to the following equation: porosity = 100 × (1-ρ1 / ρ2), where ρ1 = bulk density of β-TCP scaffold, ρ2 = theoretical density of β-TCP. The scaffolds were also characterized using X-ray diffraction (XRD, RINT2000, Rigaku, Tokyo, Japan). Cu Kα radiation at 40 kV and 20 mA was used. Diffractograms were obtained from 2θ = 20° to 50° with an increment of 0.02°, at a scanning speed of 4° / minute. Compression testing was performed on each β-TCP scaffold using a universal testing machine (Autograph AG-X, Shimadzu, Kyoto, Japan). The dimensions of each sample were 10 × 10 × 4 mm^3. The cross-head loading speed was set at 1.0 mm / min.

Cell seeding and morphology

β-TCP scaffolds were seeded with 1 × 10^4 mouse osteoblastic MC3T3-E1 cells and cultured using medium (MEM alpha-GlutaMAX-I, Life Technologies,

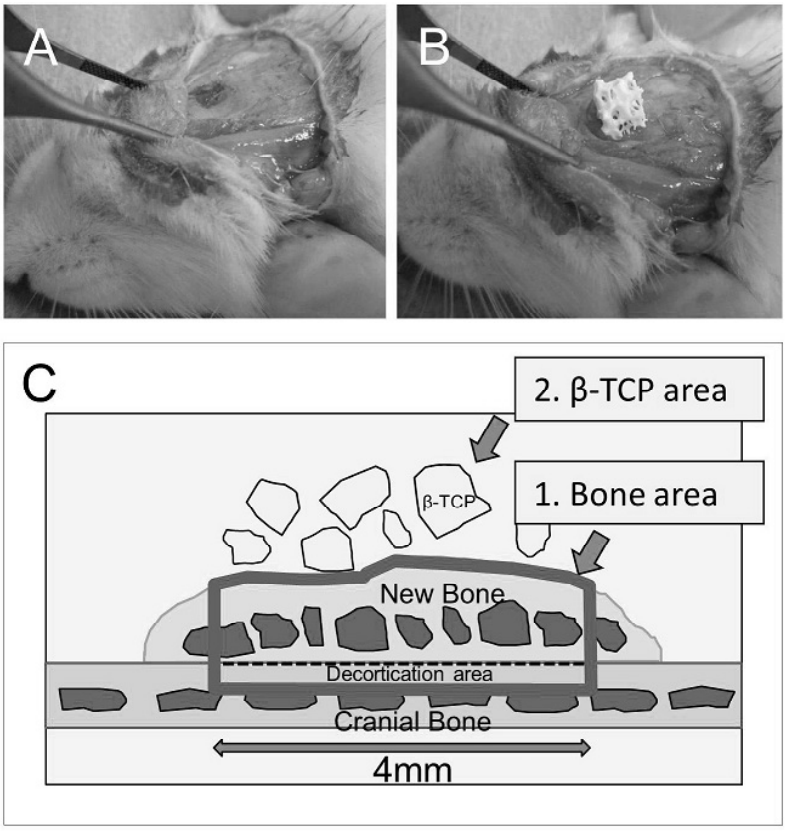

Figure 2
A) Decortication was performed in the cranial bone. B) The samples were placed on the cranial bone. C) Schematic drawing of histomorphometric analysis. The frontal plane view indicates the following parameters: the area of newly formed bone (1), the area of residual β-TCP (2).

Grand Island, NY, USA) supplemented with 10% fetal bovine serum (FBS, Qualified, Life Technologies) and 1% antibiotics (Pen Strep, Life Technologies). At 24 h of culture, sample surfaces were analyzed by SEM (S-4000, Hitachi, Tokyo, Japan) at an accelerating voltage of 10 kV after platinum coating.

Surgical procedures

Eighteen Wistar male rats (10 weeks old) were given general anesthesia with intraperitoneal injections of 0.6 ml / kg sodium pentobarbital (Somnopenthyl, Kyoritsu Seiyaku, Tokyo, Japan), and local injection of 2% lidocaine hydrochloride with 1: 80,000 epinephrine (Xylocaine cartridge for dental use, Dentsply-Sankin K.K., Tokyo, Japan). The experimental protocol followed the institutional animal use and care regulations of Hokkaido University (Animal Research Committee of Hokkaido University, Approval No. 10-42).

After a skin incision was made in the scalp, a flap was reflected. Subsequently, decortication of a 4-mm^2 area was performed in the cranial bone (Fig. 2-A). Each β-TCP scaffold specimen (6 × 6 × 5 mm) was soaked in FGF2 (FGF2 dose: 0.15 μg / μL, Fiblast® spray 500, Kaken Pharmaceutical, Tokyo, Japan) and then the β-TCP scaffold was placed on the decorticated area (Fig. 2-B). The skin was closed with nylon sutures (Softretch 4-0, GC, Tokyo, Japan) and tetracycline hydrochloride ointment (Achromycin Ointment, POLA Pharma, Tokyo, Japan) was applied to the wound.

Histological procedures and analyses

Five weeks postsurgery, the rats were euthanized using an overdose of sodium pentobarbital. Implants were excised with surrounding tissues and fixed in 10% buffered formalin. Specimens were examined by a micro X-ray CT system (R_mCT2, Rigaku, Tokyo, Japan). Subsequently, specimens were decalcified in 10% EDTA (pH 7.0) and embedded in paraffin according to standard procedures. Six-micrometer-thick sections were prepared and stained with hematoxylin and eosin and Masson's trichrome. Three stained sections were taken, one from the center of the scaffold and other two from 500 μm either side of the center, and examined using light microscopy. Histomorphometric measurements (Fig. 2-C) were performed using a software package (Image J 1.41, National Institute of Health, Bethesda, MD, USA).

Statistical analysis

The means and standard deviations of each parameter were calculated for each group. Statistical analysis was performed using the Scheffé test for structural parameters and the Games-Howell test for each histometric measurement. P-values <0.05 were considered statistically significant. All statistical procedures were performed using a software package (DR. SPSS 11.0, SPSS Japan, Tokyo, Japan).

RESULTS

Characterization of the β-TCP scaffold

Each β-TCP scaffold showed a reticulated open-cell structure (Fig. 1, 3-A). From SEM observation, cross-sections of the strut of the β-TCP scaffold revealed a tube-shaped structure (defect size: 50 μm). Many micropores with a diameter of approximately 2 μm were observed on the strut surface (Figs. 3-B, C, D). The internal space and micropores resulted from the process of dissolution and burn-up of the polyurethane foam. The cut surface of β-TCP scaffold embedded in resin showed interconnected defects within the strut of the scaffold (Figs. 3-E, F). It seems

likely that the interconnected space is advantageous for protein absorption, cell infiltration and early degradation. There were no significant differences in parameters of density and porosity of the scaffold among the three open-cell types (Table 1). The porosity was calculated to be >90% (Table 1). XRD patterns of the β-TCP scaffold are shown in Fig. 4. Only diffraction peaks belonging to β-TCP were detected among the XRD patterns from each β-TCP scaffold, indicating that pure β-TCP scaffolds had been prepared. The compressive

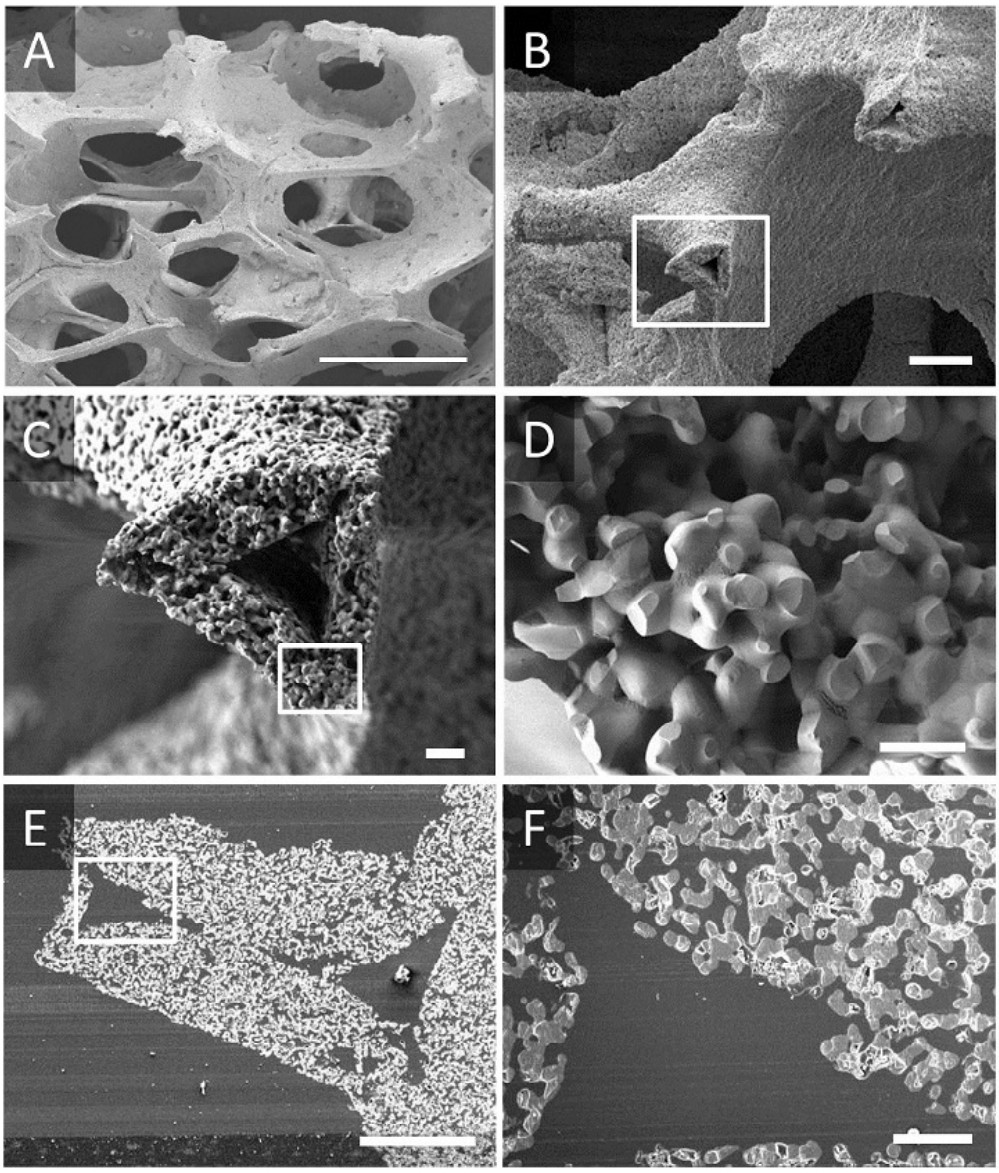

Figure 3
A) SEM micrograph of the highly porous β-TCP scaffold. B) Fracture surface of the β-TCP scaffold. C) Higher magnification of the boxed area in (B). The internal space was detected in the strut of the scaffold. Micropores were observed on the strut surface. D) Higher magnification of the boxed area in (C). Micropores were also observed at the fracture surface of the strut. E) Cut surface of the strut of the β-TCP scaffold. F) Higher magnification of the boxed area in (E). Interconnection between internal space and micropores is exhibited. Scale bars represent 1 mm (A), 100 μm (B, E), 10 μm (C, F) and 5 μm (D).

strength of the 0.6-mm and 0.4-mm cell type scaffolds was significantly higher than that of 0.3-mm type (Table 1). Osteoblastic MC3T3-E1 cells attached and spread on the β-TCP scaffold, suggesting that the scaffold possesses good cyto-compatibility (Fig. 5-A).

Histological observations

Bone augmentation was stimulated by FGF2-loaded β-TCP scaffold implantation. X-ray CT imaging showed the radiodense enlargement continuous with the pre-existing bone (Fig. 5-B). New bone was frequently found in the interior of the β-TCP scaffold. In the 0.4-mm cell size scaffold, considerable bone formation was clearly detectable (Figs 6-A, B, C).

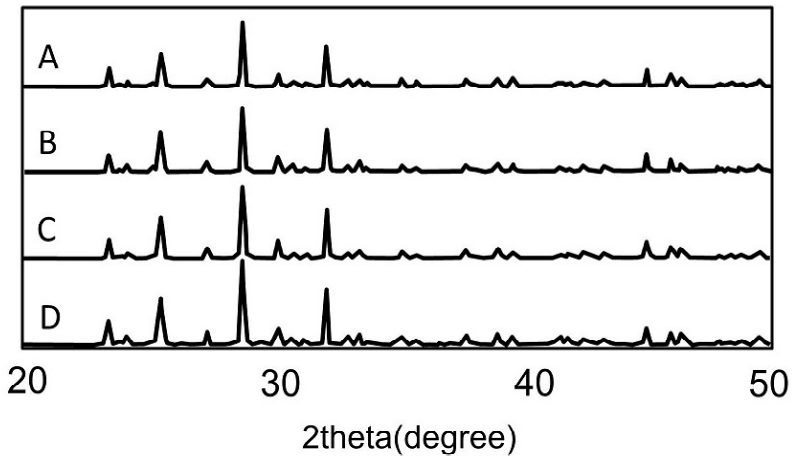

Figure 4
XRD patterns of β-TCP scaffolds with different cell types: 0.6 (A), 0.4 (B), 0.3 (C) mm, and β-TCP powder (D).

Table 1 Structural parameters of β-TCP scaffold (N = 6, mean ± SD)

Open-cell size	0.6-mm	0.4-mm	0.3-mm
Density (g / cm^3)	0.16 ± 0.03	0.20 ± 0.04	0.19 ± 0.02
Porosity (%)	94.7 ± 0.8	93.5 ± 1.3	93.7 ± 0.5
Compressive strength (MPa)	0.024 ± 0.001 [a]	0.023 ± 0.006 [a]	0.009 ± 0.004

[a] Statistical difference compared to 0.3-mm cell type.

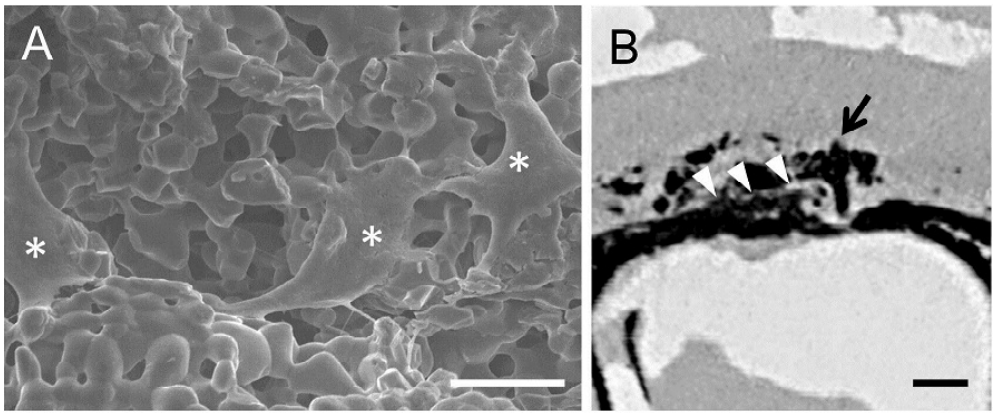

Figure 5
A) SEM micrograph of MC3T3-E1 cells seeded on the β-TCP scaffold. Cell attachment and spreading are shown on the scaffold (stars). B) X-ray CT Image. Radiographic signs of bone augmentation (arrowheads) and residual material (arrow) are presented. Scale bars represent 10 μm (A) and 1 mm (B).

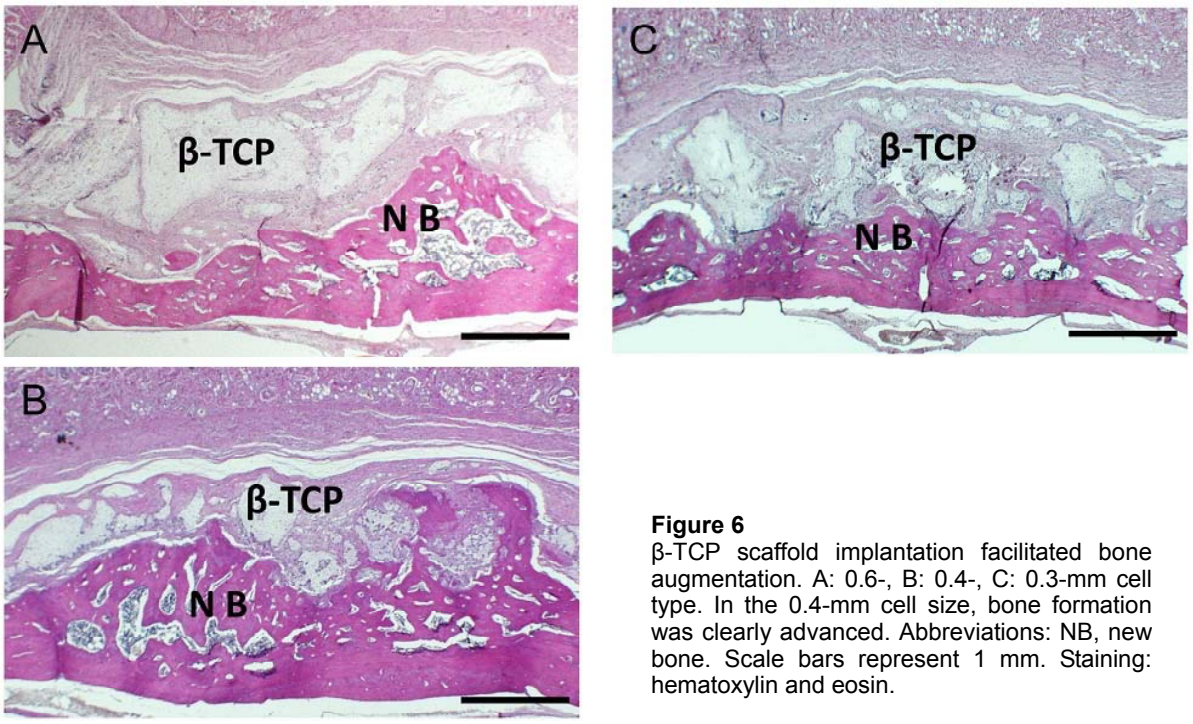

Figure 6
β-TCP scaffold implantation facilitated bone augmentation. A: 0.6-, B: 0.4-, C: 0.3-mm cell type. In the 0.4-mm cell size, bone formation was clearly advanced. Abbreviations: NB, new bone. Scale bars represent 1 mm. Staining: hematoxylin and eosin.

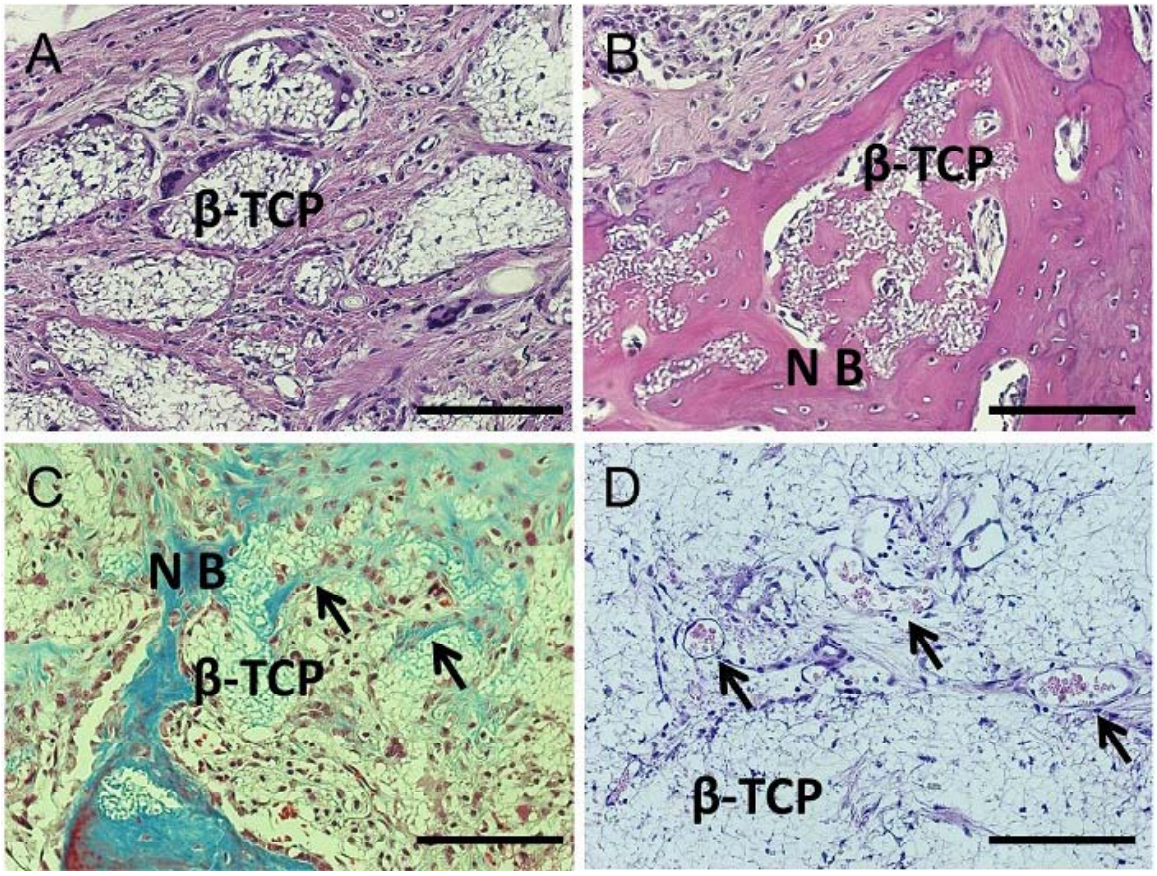

Figure 7
A) Giant cells were observed close to residual β-TCP. B) Bone in-growth was frequently demonstrated. C) Ingrowth of connective tissue (arrows) was also observed. D) Blood vessels (arrows) were detected in the residual β-TCP scaffold strut. Abbreviations: NB, new bone. Scale bars represent 100 μm. Staining: hematoxylin and eosin (A, B, D) and Masson's trichrome (C).

Residual β-TCP was detected around the new bone tissue and was frequently encapsulated by cell-rich connective tissue including giant cells, suggesting that resorption of β-TCP and osteogenesis occurred simultaneously (Fig. 7-A). The β-TCP scaffold seemed to allow tissue in-growth: bone-like tissue formed at the inner space of the β-TCP strut of the scaffold (Figs. 7-B, C). Blood vessels were also formed in the residual β-TCP strut (Fig. 7-D). These events might be associated with the interconnected structure of the β-TCP scaffold and FGF2 loading. Few inflammatory cells were seen around the residual material, indicating that the material possessed high biocompatibility.

Histomorphometric analysis

The histomorphometric analysis data for each material are presented in Table 2. The β-TCP scaffold with the 0.4-mm cell size had the highest osteoconductivity among all groups. Regarding bone area measurement, the 0.4-mm cell size was significantly greater than the 0.6- and 0.3-mm cell sizes. Furthermore, the 0.6-mm type scaffold significantly facilitated bone formation compared to the 0.3-mm type. Resorption of the β-TCP scaffold with the 0.4-mm cell size scaffold was frequently accelerated. The residual material area in 0.4-mm cell size was significantly lower compared with 0.6- and 0.3-mm cell sizes.

DISCUSSION

The regeneration scaffold is a major element of tissue engineering that allows attachment, repopulation and differentiation of cells. In addition, the morphology and the structure of the scaffold can regulate biological reactions [19, 20]. Scaffolds for bone tissue engineering should be designed to mimic native bone structure so that they can integrate into the surrounding bone tissue [21]. In this experiment, a β-TCP scaffold was made from template polyurethane foam using a structure with a larger inner space; the scaffold had high porosity and interconnectivity, much like trabecular bone.

This study examining different β-TCP scaffolds revealed that the biological response to implantation is influenced by open-cell size. Bone formation was facilitated by each β-TCP scaffold sample. However, the fastest bone augmentation and ceramic resorption occurred in the 0.4-mm cell size. Many studies have demonstrated that bone in-growth is affected by the morphology of the materials [17, 18]. In this study, we speculated that the similarity of the scaffold morphology to native trabecular bone might be related to bone formation. Mature bone includes around 1.0-mm-sized pores within the marrow, while newly formed woven bone has a smaller pore size (<0.5 mm) [13, 22]. Therefore, 0.4- and 0.3-mm cell type scaffolds were considered to be morphologically suitable for early bone reformation.

Table 2 Histomorphometric analysis after β-TCP scaffold implantation (N = 6, mean ± SD).

Open-cell size	0.6-mm	0.4-mm	0.3-mm
Bone area (mm^2)	2.75 ± 0.54 [ab]	3.78 ± 0.58 [a]	1.24 ± 0.69
β-TCP area (mm^2)	2.83 ± 0.76 [b]	1.12 ± 0.29	3.08 ± 0.36 [b]

[a] Statistical difference compared to 0.3-mm cell type.
[b] Statistical difference compared to 0.4-mm cell type.

Osteogenesis is associated with other parameters of the scaffold, such as density, interconnected structure and stability [19]. The mechanical properties of the regenerative scaffold play a facilitative role in maintaining the regenerative space following application to the body [1]. It was revealed that the 0.6- and 0.4-mm cell sized scaffolds had high compressive strength compared to the 0.3-mm type. The structure of the polyurethane foam affected the stability of the β-TCP scaffold; the low compressive strength in 0.3-mm type was presumably caused by slender struts. The 0.3-mm type would be compressed early after implantation and not maintain the cell-invading and regenerative space. In future, it will be necessary to examine the strut structure of highly porous β-TCP scaffolds.

Application of β-TCP induces phagocytosis by macrophages[23]. In this study, many giant cells resembling macrophages were observed close to β-TCP struts, suggesting that a high local calcium concentration was maintained by β-TCP resorption. Calcium ions released by β-TCP degradation stimulate the alkaline phosphatase activity of osteoblastic cells [24]. It seems likely that higher ion exchange by degradation of the 0.4-mm cell type scaffold additionally enhances bone formation. On the other hand, FGF2 induces biological responses in relation to wound healing [12]. Formation of new bone is prominently stimulated by FGF2 loading [13-15]. Therefore, implantation of highly porous β-TCP scaffolds with FGF2 provides a favorable environment for osteogenesis.

We conclude that bone augmentation is promoted by morphology and regenerative space maintenance associated with 0.4-mm open-cell sized β-TCP scaffolds. FGF2-loaded β-TCP scaffolds are expected to provide a suitable material for bone tissue engineering.

ACKNOWLEDGMENTS

We thank Tomita Pharmaceuticals Co., Ltd., for providing the β-TCP. This work was supported by JPSP KAKENHI Grant Number 22791916. None of the authors have any conflicts of interest associated with this study.

REFERENCES

1) Liu X, Rahaman MN, Fu Q. Bone regeneration in strong porous bioactive glass (13-93) scaffolds with an oriented microstructure implanted in rat calvarial defects. Acta Biomater 2013; 9:4889-4898.
2) Yoshikawa M, Tsuji N, Shimomura Y, Hayashi H, Ohgushi H. Osteogenesis depending on geometry of porous hydroxyapatite scaffolds. Calcif Tissue Int 2008; 83:139-145.
3) Fujita R, Yokoyama A, Kawasaki T, Kohgo T. Bone augmentation osteogenesis using hydroxyapatite and beta-tricalcium phosphate blocks. J Oral Maxillofac Surg 2003; 61:1045-1053.
4) Sohier J, Daculsi G, Sourice S, de Groot K, Layrolle P. Porous beta tricalcium phosphate scaffolds used as a BMP-2 delivery system for bone tissue engineering. J Biomed Mater Res A 2010; 92:1105-1114.
5) Chuenjitkuntaworn B, Inrung W, Damrongsri D, Mekaapiruk K, Supaphol P, Pavasant P. Polycaprolactone / hydroxyapatite composite scaffolds: preparation, characterization, and in vitro and in vivo biological responses of human primary bone cells. J Biomed Mater Res A 2010; 94:241-251.
6) Lan Levengood SK, Polak SJ, Poellmann MJ, Hoelzle DJ, Maki AJ, Clark SG, Wheeler MB, Wagoner Johnson AJ. The effect of BMP-2 on micro- and macroscale osteointegration of biphasic calcium phosphate scaffolds with multiscale porosity. Acta Biomater 2010; 6:3283-3291.
7) Ogose A, Hotta T, Kawashima H, Kondo N, Gu W, Kamura T, Endo N. Comparison of hydroxyapatite and beta tricalcium phosphate as bone substitutes after excision of bone tumors. J Biomed Mater Res B Appl Biomater 2005;72:94-101.
8) Sarment DP, Cooke JW, Miller SE, Jin Q, McGuire MK, Kao RT, McClain PK, McAllister BS, Lynch SE, Giannobile

WV. Effect of rhPDGF-BB on bone turnover during periodontal repair. J Clin Periodontol 2006;33:135-140.
9) Oi Y, Ota M, Yamamoto S, Shibukawa Y, Yamada S. β-tricalcium phosphate and basic fibroblast growth factor combination enhances periodontal regeneration in intrabony defects in dogs. Dent Mater J 2009; 28:162-169.
10) Gaasbeek RD, Toonen HG, van Heerwaarden RJ, Buma P. Mechanism of bone incorporation of β-TCP bone substitute in open wedge tibial osteotomy in patients. Biomaterials 2005; 26: 6713-6719.
11) Stavropoulos A, Windisch P, Szendröi-Kiss D, Peter R, Gera I, Sculean A. Clinical and histologic evaluation of granular beta-tricalcium phosphate for the treatment of human intrabony periodontal defects: a report on five cases. J Periodontol 2010; 81:325-334.
12) Yun YR, Won JE, Jeon E, Lee S, Kang W, Jo H, Jang JH, Shin US, Kim HW. Fibroblast growth factors: biology, function, and application for tissue regeneration. J Tissue Eng 2010;2010: 218142.
13) Kobayashi N, Miyaji H, Sugaya T, Kawanami M. Bone augmentation by implantation of an FGF2-loaded collagen gel-sponge composite scaffold. J Oral Tissue Engin 2010; 8: 91-101.
14) Canalis E, Centrella M, McCarthy T. Effects of basic fibroblast growth factor on bone formation in vitro. J Clin Invest 1998; 81:1572-1577.
15) Fei Y, Xiao L, Doetschman T, Coffin DJ, Hurley MM. Fibroblast Growth Factor 2 Stimulation of osteoblast differentiation and bone formation is mediated by modulation of the wnt signaling pathway. J Biol Chem 2011; 286:40575–40583.
16) Roy TD, Simon JL, Ricci JL, Rekow ED, Thompson VP, Parsons JR. Performance of degradable composite bone repair products made via three-dimensional fabrication techniques. J Biomed Mater Res A 2003; 66: 283–291.
17) Tsuruga E, Takita H, Itoh H, Wakisaka Y, Kuboki Y. Pore size of porous hydroxyapatite as the cell-substratum controls BMP induced osteogenesis. J Biochem 1997; 121:317–324.
18) Kasten P, Beyen I, Niemeyer P, Lugin-bühl R, Bohner M, Richter W. Porosity and pore size of beta-tricalcium phos-phate scaffold can influence protein production and osteogenic differentiation of human mesenchymal stem cells: an in vitro and in vivo study. Acta Biomater 2008; 4:1904-1915.
19) Kasten P, Luginbühl R, van Griensven M, Barkhausen T, Krettek C, Bohner M, Bosch U. Comparison of human bone marrow stromal cells seeded on calcium-deficient hydroxyapatite, beta-tricalcium phosphate and demineralized bone matrix. Biomaterials 2003;24: 2593-2603.
20) Yeo A, Wong WJ, Khoo HH, Teoh SH. Surface modification of PCL-TCP scaffolds improve interfacial mechanical interlock and enhance early bone formation: an in vitro and in vivo characterization. J Biomed Mater Res A. 2010; 92: 311-321.
21) Karageorgiou V, Kaplan D. Porosity of 3D biomaterial scaffolds and osteogenesis. Biomaterials 2005; 26:5474–5491.
22) Kosen Y, Miyaji H, Kato A, Sugaya T, Kawanami M. Application of collagen hydrogel / sponge scaffold facilitates periodontal wound healing in class II furcation defects in beagle dogs. J Periodont Res 2012; 47:626–634.
23) Nagayama M, Takeuchi H, Doi Y. Comparison of carbonate apatite and beta-tricalcium phosphate (resorbable calcium phosphates) implanted subcutaneously into the back of rats. Dent Mater J 2006; 25:219-225.
24) Xia L, Zhang Z, Chen L, Zhang W, Zeng D, Zhang X, Chang J, Jiang X. Proliferation and osteogenic differentiation of human periodontal ligament cells on akermanite and β-TCP bioceramics. Eur Cell Mater 2011;22:68-82; discussion 83.

(Received, February 4, 2013/
Accepted, March 26, 2013)

Corresponding author:
Dr. Hirofumi MIYAJI, D.D.S.,Ph.D
Department of Periodontology and Endodontology,
Hokkaido University Graduate School of Dental Medicine. N13 W7 Kita-ku, Sapporo 060-8586, Japan.
Tel: +81 11 706 4266
Fax: +81 11 706 4334
E-mail : miyaji@den.hokudai.ac.jp